Asian Journal of Andrology (2023) 25, 322–330
www.asiaandro.com; www.ajandrology.com

Open Access

ORIGINAL ARTICLE

Male Infertility

FOXP4 promotes proliferation of human spermatogonial stem cells

Shu-Wei Luo[1,2,*], Le Tang[1,2,*], Dai Zhou[3,4], Hao Bo[3,4], Li-Qing Fan[3,4]

Continuous self-renewal and differentiation of spermatogonial stem cells (SSCs) is vital for maintenance of adult spermatogenesis. Although several spermatogonial stem cell regulators have been extensively investigated in rodents, regulatory mechanisms of human SSC self-renewal and differentiation have not been fully established. We analyzed single-cell sequencing data from the human testis and found that forkhead box P4 (FOXP4) expression gradually increased with development of SSCs. Further analysis of its expression patterns in human testicular tissues revealed that FOXP4 specifically marks a subset of spermatogonia with stem cell potential. Conditional inactivation of FOXP4 in human SSC lines suppressed SSC proliferation and significantly activated apoptosis. FOXP4 expressions were markedly suppressed in tissues with dysregulated spermatogenesis. These findings imply that FOXP4 is involved in human SSC proliferation, which will help elucidate on the mechanisms controlling the fate decisions in human SSCs.
Asian Journal of Andrology (2023) **25**, 322–330; doi: 10.4103/aja202254; published online: 19 August 2022

Keywords: forkhead box P4; human; proliferation; spermatogonial stem cells; testis

INTRODUCTION

Globally, infertility affects about 15% of couples of childbearing age, with male factors contributing to about 50% of infertility cases.[1] Assisted reproductive technologies such as intracytoplasmic sperm injection (ICSI) have overcome most of the challenges to male infertility. However, nonobstructive azoospermia (NOA) remains a major cause of infertility,[2] and owing to its complex pathogenesis, lacks effective treatment options.

Spermatogonial stem cells (SSCs), which undergo spermatogenesis, have been shown to restore natural reproduction in mice.[3] However, because of significant differences between human and rodent SSCs, findings from mouse studies may not accurately reflect the functions of human SSCs.[4] Thus, studies involving human SSCs should be performed to indicate strategies for restoring male fertility. SSCs are localized near the basement membrane of seminiferous tubules, where they initiate and maintain spermatogenesis.[5] The development of SSC is influenced by the extracellular microenvironment and intracellular factors. Defects in spermatogenesis may lead to spermatogenic failure, resulting in male infertility.[6] A recent review involving animal models has reported some of the mechanisms regulating SSC development.[7] Glial cell line-derived neurotrophic factor (GDNF) is a key factor in regulation of SSC self-renewal.[8] *In vitro*, fibroblast growth factor 2 (FGF2) and GDNF separately enhanced SSC self-renewal and proliferation. However, these two proteins have distinct functions, with FGF2 promoting differentiation and GDNF enhancing stemness.[9] The reasons for these differences have not been established. Both GDNF and FGF2 lead to activation of several signaling pathways, such as mitogen-activated protein kinase (MAPK), rat sarcoma (RAS)/extracellular regulated protein kinases (ERK), and phosphoinositide 3-kinase (PI3K)/serine/threonine-protein kinase akt (AKT).[10-12] These pathways enhance SSC self-renewal by upregulating many genes including ETS translocation variant 5 (*Etv5*),[13] B-cell CLL/lymphoma 6 member B (*Bcl6b*),[13] LIM homeobox protein 1 (*Lhx1*),[14] T-box transcription factor T (*T*),[15] and C-X-C motif chemokine receptor 4 (*Cxcr4*).[16] Additionally, such growth factors as epidermal growth factor (EGF), wingless-related murine mammary tumor virus (MMTV) integration site genes (WNT), and leukemia inhibitory factor (LIF) can affect SSC self-renewal as well as differentiation.[17] Endogenous factors, including promyelocytic leukemia zinc finger (PLZF), play key functions in maintenance of SSC self-renewal.[18] PLZF can antagonize sal-like protein 4 (SALL4) regulated SSC differentiation.[19] Moreover, PLZF and GDNF coregulate several signaling molecules, which enhances SSC self-renewal, promoting effects of GDNF.[20] Deficiencies in PLZF result in a gradual loss of germ cells, leading to infertility.[18]

However, owing to biological and classification differences between human and mouse SSCs, findings from murine models cannot be fully extended to humans.[6] In mice, undifferentiated cells are generally divided into single (A_s), pair (A_{pr}), and chain (A_{al}) spermatogonia.[17,21] A_s are considered to be true SSCs.[22] Under appropriate conditions, A_{pr} and A_{al} re-enter the A_s through syncytial fragmentation.[23] In humans, from the degree of hematoxylin staining and the morphological characteristics of the nuclei,[6,24] SSCs are classified as dark stained (A_{dark}) or light stained (A_{pale}). With regard to the combinations and morphology of spermatogenic cells, the spermatogenic process in mice is divided into 12 stages, whereas in humans, there are only six.[25,26] In

[1]Reproductive Medicine Center, Hunan Provincial Maternal and Child Health Care Hospital, Changsha 410000, China; [2]NHC Key Laboratory of Birth Defect for Research and Prevention, Hunan Provincial Maternal and Child Health Care Hospital, Changsha 410000, China; [3]Institute of Reproduction and Stem Cell Engineering, School of Basic Medicine Science, Central South University, Changsha 410000, China; [4]Reproductive and Genetic Hospital of CITIC-Xiangya, Changsha 410000, China.
*These authors contributed equally to this work.
Correspondence: Dr. LQ Fan (801646@csu.edu.cn)
Received: 27 March 2022; Accepted: 01 July 2022

addition, human and mouse SSCs exhibit numerous different molecular markers. For instance, GDNF family receptor alpha 1 (GFRA1), a conventional SSC marker, labels a very small proportion of mouse spermatogonia but is abundant in human spermatogonia.[6] Another marker, octamer-binding protein 4 (OCT4), is present in mouse SSCs but not in human SSCs.[27,28] F-Box and WD repeat domain-containing-7 (FBXW7) is only expressed in undifferentiated mouse spermatogonia but broadly expressed in human spermatogonia.[29,30] Thus, given these differences in developmental regulatory mechanisms of SSCs, human tissues and cells are more suitable for studying human SSCs.

Single-cell RNA sequencing (scRNA-seq) can identify genes involved in SSC fate determination at single-cell resolution. We analyzed testicular scRNA-seq datasets (GSE149512[31] and GSE112013[32]) to identify genes associated with SSC development and found that forkhead box P4 (FOXP4) was specifically expressed in human SSCs, and its expressions gradually increased with SSC development. The *FOXP4* gene, a member of the FOXP family of transcription factors, plays a role in embryonic development, immune regulation, as well as tumor growth.[33] It is mainly expressed in embryonic lungs, nerves, and intestinal tissues.[34] Expressions of these genes partially overlap, and together, they form a large multi-domain transcription factor.[35,36] However, in some cases, FOXP4 functions independently. For instance, FOXP4 promotes the progression of various tumors, such as liver[37] and breast cancers[38] as well as esophageal squamous cell carcinoma.[39] It also regulates forebrain development and neuroepithelial characteristics and maintains progenitor cells in the central nervous system by inhibiting N-cadherin.[34] Moreover, it is essential in the maintenance of cerebellar Purkinje cell arborization.[40]

In this study, we found that FOXP4 was mainly expressed in human SSCs. FOXP4 deficiency significantly reduced cell proliferation and promoted apoptosis. In addition, FOXP4 expression was significantly suppressed in testicular tissues with dysregulated spermatogenesis, implying that FOXP4 regulates human spermatogenesis by maintaining SSC viabilities. We revealed the role of FOXP4 in regulating SSC fate and functions, which provided a target for diagnosis and treatment of male infertility.

MATERIALS AND METHODS

Identification of cell types and clustering analyses

The Seurat program (R package, version 3.0; http://satijalab.org/seurat/) was used to analyze scRNA-seq datasets of eight adult testes with normal spermatogenesis, GSE149512 (5 samples) and GSE112013 (3 samples). First, expression matrix data were loaded onto R using the Read.table or Read.csv function after which Seurat objects were developed from each assay. Each assay was filtered and normalized with default settings. Only cells expressing >500 genes and with <20% of reads mapped to the mitochondrial genome were retained. After identification of the variable features of each object, all data were merged using the IntegrateData function. Mitochondrial and ribosomal genes were removed, and then, Uniform Manifold Approximation and Projection (UMAP) and clustering were analyzed on the combined datasets of the top 2500 highly variable genes and PCs 1–13. Next, deeper SSC clustering identified two subclusters. Subsequently, SSCs from the UMAP plot were subjected to pseudotime assessment via "Monocle" in R (version 3.0; https://cole-trapnell-lab.github.io/monocle3/) starting with the subcluster at State 0. Heatmaps were established in pseudotime order, with plotting of line plots done in a pseudotime order and curves fitted using the "auto" method of "ggplot2" in R (https://ggplot2.tidyverse.org/).

Human testicular tissue collection

Ethical approval for this study was obtained from the Hunan Provincial Maternal and Child Health Care Hospital (Changsha, China; No. 2021-S086), and all participants provided written informed consent. Samples were obtained from NOA and obstructive azoospermia (OA) patients subjected to testicular biopsy. Patients with known genetic defects, such as Y chromosome microdeletions and Klinefelter syndrome, were excluded. Testicular tissues (weighing between 10 mg and 20 mg) were obtained from 20 patients aged 26–52 years. On the basis of hematoxylin and eosin (H&E) staining (Beyotime, Shanghai, China) analysis, samples were classified as normal, Sertoli cell-only syndrome (SCOS), spermatogonial arrest, or spermatocyte arrestor hypospermatogenesis. Tissues were washed thrice with phosphate buffered saline (PBS) and fixed in 4% paraformaldehyde (PFA) or frozen in liquid nitrogen.

Culturing of human spermatogonial stem cell lines

The human spermatogonial stem cell line, developed as described by Hou *et al*.,[41] was a gift from Prof. Zuping He of Hunan Normal University (Changsha, China). Cells were cultured in Dulbecco's Modified Eagle Media: nutrient mixture F-12 (DMEM/F12; Gibco, Grand Island, NY, USA) supplemented with 10% fetal bovine serum (FBS; Gibco) and 100 units of penicillin/streptomycin (Invitrogen, Carlsbad, CA, USA) at 34°C in the 5% CO_2 atmosphere. Cells were passaged after every 3 days with 0.05% trypsin-ethylenediaminetetraacetic acid (EDTA; Invitrogen).

RNA extraction and real-time quantitative polymerase chain reaction (RT-qPCR)

An RNAiso Plus kit (Takara, Kusatsu, Japan) was used for isolating total RNA. The concentration and quality of extracted RNA were evaluated using Nanodrop (Thermo Scientific, Waltham, MA, USA). Next, it was reverse-transcribed into cDNA using the First Strand cDNA synthesis kit (Thermo Scientific). Samples were subjected to qPCR analyses with SYBR Premix Ex Taq II (Takara) on an Applied Biosystems ABI Prism 7700 system (Applied Biosystems, Foster City, CA, USA), as instructed by the manufacturer. Relative gene expressions were calculated by using the $2^{-\triangle\triangle Ct}$ method. Beta-actin (*ACTB*) was used as the reference gene. Each sample was analyzed in triplicate. Primer sequences are shown in **Supplementary Table 1**.

Protein extraction and Western blot analysis

Testicular samples and human SSCs were incubated in the Radio-Immunoprecipitation Assay (RIPA) lysis buffer (Thermo Scientific) for 30 min on ice and centrifuged (Centrifuge 5418 R, Eppendorf, Hamburg, Germany) at 12 000*g* for 15 min. The bicinchoninic acid (BCA) assay kit (Thermo Scientific) was used to determine protein concentrations, after which 20 μg of each protein sample was separated on sodium dodecyl sulfate polyacrylamide gel electrophoresis (SDS-PAGE; Bio-Rad, Hercules, CA, USA) and subjected to Western blot.[42] The antibodies used in this assay are listed in **Supplementary Table 2**. Protein bands were visualized by the chemiluminescence system (Bio-Rad).

Immunohistochemistry and immunofluorescence

For immunohistochemistry, xylene was used for deparaffinizing testis sections. Samples were rehydrated using graded ethanol and heated in 0.01 mol l^{-1} sodium citrate buffer at 98°C for 18 min for antigen retrieval. Then, endogenous peroxidase activities were blocked with 3% H_2O_2 (Zsbio, Beijing, China) after which tissues were permeabilized by incubating with 0.25% Triton X-100 (Sigma, Steinheim, Germany) for 15 min. Tissues were blocked for 1 h using 5% goat serum at room temperature, incubated overnight with primary antibodies (**Supplementary Table 2**) at

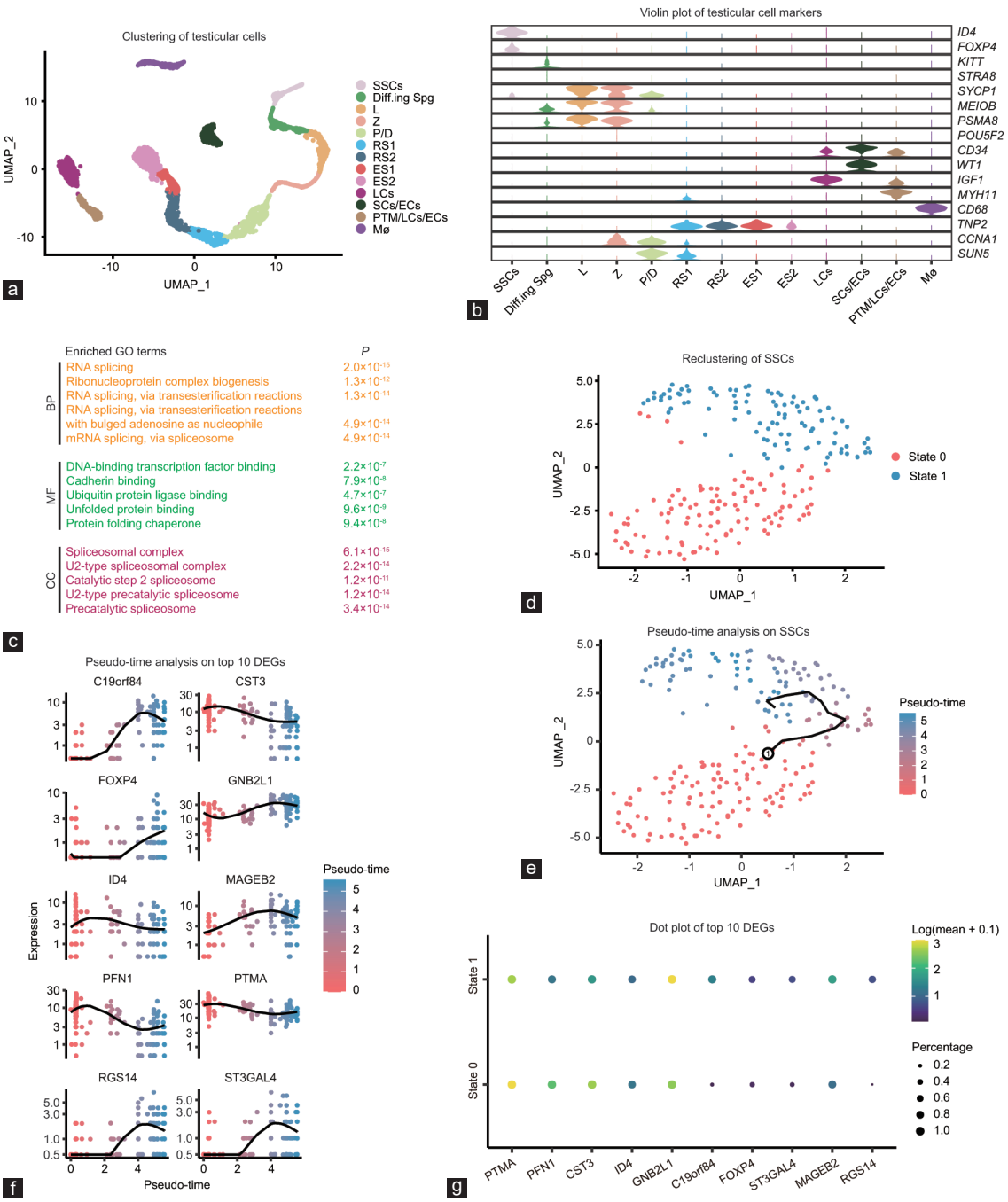

Figure 1: Integrated analysis of human testes single-cell sequencing datasets (GSE149512 and GSE112013). (**a**) UMAP and clustering analyses of combined single-cell transcriptomic data from human testes. (**b**) Violin plots showing expression patterns of various markers. (**c**) Enriched GO terms and *P* values of SSC clusters. (**d**) UMAP and reclustering analysis of SSC clusters. (**e**) Pseudotime analysis of SSCs cluster showing two discrete cellular states (States 0 and 1) during SSC development. (**f**) Expression levels of the top 10 DEGs during SSC development. The x-axis denotes pseudotime (as defined in **e**); the y-axis denotes gene expression levels. (**g**) Dot plot for the top 10 DEGs in States 0 and 1. Yellow indicates elevated levels while blue indicates suppressed or no expression. The size of each circle represents the positive percentage of each gene. SSCs: spermatogonial stem cells; Diff.ing Spg: differentiating spermatogonia; L: leptotene spermatocytes; Z: zygotene spermatocytes; P/D: pachytene/diplotene spermatocytes; RS: round spermatids; ES: elongated spermatids; LCs: Leydig cells; SCs: Sertoli cells; ECs: endothelial cells; PTM: peritubular myoid cells; Mø: macrophages; GO: gene ontology; DEGs: differentially expressed genes; UMAP: Uniform Manifold Approximation and Projection; BP: biological process; MF: molecular function; CC: cellular component.

4°C, washed in PBS, and incubated with horseradish peroxidase (HRP)-conjugated secondary antibodies for 1 h at room temperature. Signals were developed with a diaminobenzidine (DAB) chromogen kit (Dako, Glostrup, Denmark). Sections were counterstained with hematoxylin. For immunofluorescence, tissue sections were incubated with Alexa Fluor conjugated–secondary antibodies for 1 h at room temperature followed by nuclei counterstaining with 4',6-diamidino-2-phenylindole (DAPI). Finally, they were examined and imaged in a Zeiss microscope (Carl Zeiss, Oberkochen, Germany).

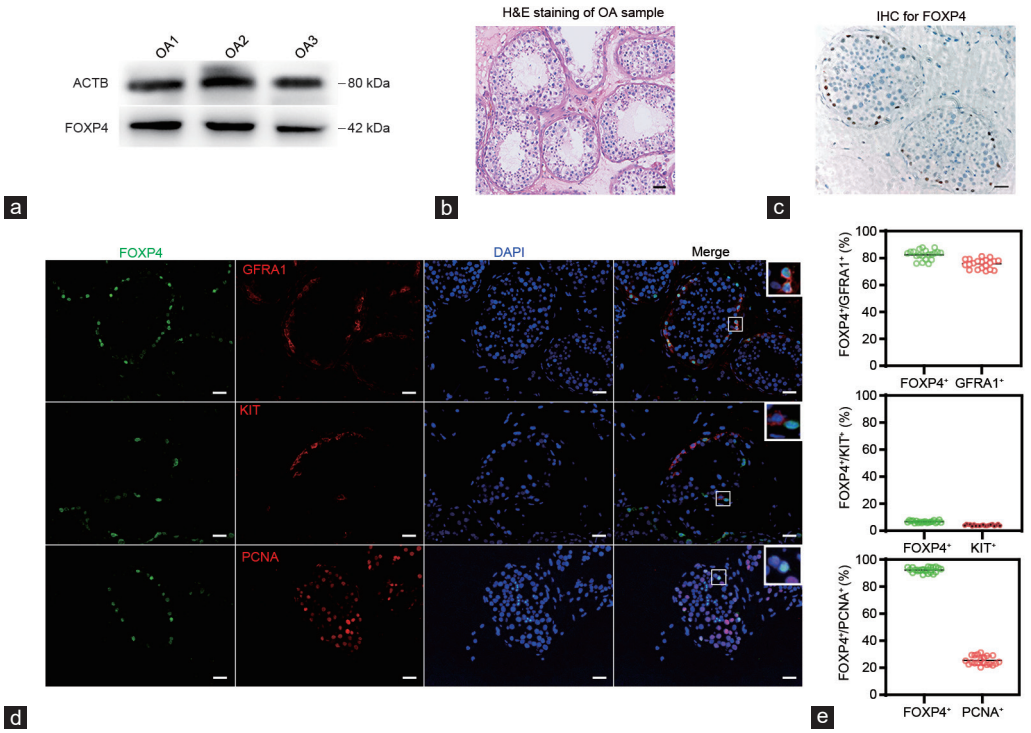

Figure 2: FOXP4 as a specific marker for human spermatogonial stem cells. (**a**) Western blot results showing FOXP4 levels in three OA samples with normal spermatogenesis. (**b**) Representative H&E image of OA testicular tissues. (**c**) Immunohistochemistry images for cell localization of FOXP4 in OA sample. (**d**) Double immunostaining revealing coexpressions of FOXP4 and GFRA1, KIT, and PCNA in human testis with normal spermatogenesis. (**e**) Abundance of FOXP4+ cells coexpressing GFRA1, KIT, and PCNA. The y-axis represents the percentage of double-positive cells. At least 20 seminiferous tubules were assessed. Scale bars = 50 μm in **b**–**d**. FOXP4: forkhead box P4; GFRA1: GDNF family receptor alpha 1; KIT: KIT proto-oncogene, receptor tyrosine kinase; PCNA: proliferating cell nuclear antigen; FOXP4: forkhead box P4; ACTB: beta-actin; OA: obstructive azoospermia; H&E: hematoxylin and eosin; IHC: immunohistochemistry; DAPI: 4',6-diamidino-2-phenylindole.

Gene knockdown

FOXP4 small interfering RNA (siRNA; **Supplementary Table 3**) and scrambled negative control siRNAs were bought from Ribobio (Guangzhou, China). Human SSCs were transfected with siRNA (100 nmol l^{-1}) using the lipofectamine 3000 reagent (Life Technologies, Carlsbad, CA, USA), as instructed by the manufacturer. After 48 h, cells were harvested for determination of mRNA and protein levels.

Cell counting kit-8 (CCK-8) assay

The proliferation rate of SSCs was determined with the CCK-8 assay kit (Dojindo, Kumamoto, Japan). Briefly, 10% CCK-8 reagent was added to the culture media of SSCs and incubated for 3 h. Absorbance (450 nm) of the media was read on a microplate reader (Thermo Scientific).

The 5-ethynyl-2'-deoxyuridine (EdU) incorporation assay

Human SSCs were inoculated on 96-well plates at 5000 cells per well in DMEM/F12 media containing 50 μmol l^{-1} EdU (RiboBio). After incubation for 12 h, cells were washed with DMEM and fixed in 4% PFA. Cells were neutralized in glycine (2 mg ml^{-1}), followed by permeabilization for 10 min with 0.5% Triton X-100 at room temperature. The EdU staining results were visualized with an Apollo staining reaction buffer. Cell nuclei were counterstained with Hoechst 33342 and examined by fluorescence microscopy (Carl Zeiss). The EdU positivity rate was determined by counting ≥500 cells.

Flow cytometry with Allophycocyanin-conjugated Annexin V/propidium iodide (Annexin V-APC/PI) staining

Human SSCs transfected with *FOXP4*-siRNA were digested and rinsed twice using ice-cold PBS; 10^6 cells were resuspended in Annexin V binding buffer (BD Biosciences, San Jose, CA, USA), as instructed by the manufacturer. This was followed by incubation with 5 μl APC-labeled Annexin V and 10 μl PI solution for 15 min at room temperature in the dark. A C6 flow cytometer (BD Biosciences) was used for the analyses.

Terminal deoxynucleotidyl transferase (TdT)-mediated dUTP nick-end labeling (TUNEL) assay

An *in situ* cell death detection kit (Roche, Mannheim, Germany) was used to evaluate the apoptosis of human SSCs transfected with *FOXP4* siRNAs, according to the manufacturer's instructions. Cells were incubated with proteinase K (20 mg ml^{-1}) for 15 min at room temperature followed by incubation with a dUTP labeling/TdT enzyme buffer for 1 h in the dark. Nuclei were counterstained with DAPI. Cells incubated with PBS and without the TdT enzyme were used as negative controls. In each sample, at least 500 cells were evaluated in a Zeiss fluorescence microscope.

Statistical analyses

Data were analyzed using GraphPad Prism 8.0 (GraphPad Software, La Jolla, CA, USA). Data are shown as mean ± standard deviation (s.d.). Data distribution was tested by D'Agostino and Pearson and Shapiro–Wilk normality test to establish the type of statistical tests (parametric or nonparametric). Wilcoxon matched-pairs signed rank test was used to calculate the statistical difference of TUNEL-positive cells, for other data, Student's *t*-test was used to calculate statistical difference. $P < 0.05$ indicated statistical significance.

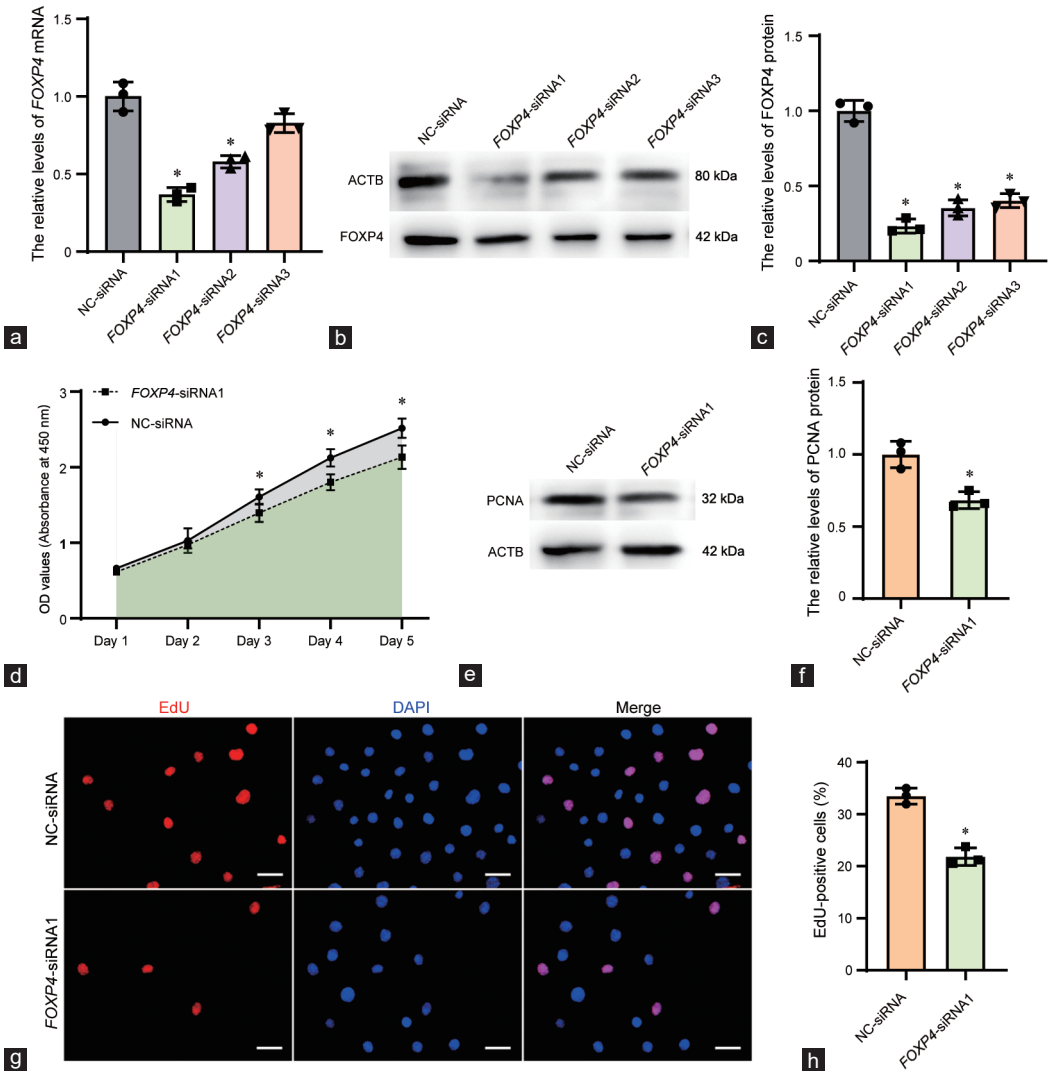

Figure 3: Effects of FOXP4 inhibition on proliferation of human SSCs. (**a**) RT-qPCR results showing *FOXP4* mRNA levels in a human SSC line after transfection with *FOXP4*-siRNA1, 2, and 3. (**b**) Western blot for FOXP4 protein expression in the human SSC line after transfection with *FOXP4*-siRNA1, 2, and 3. The ACTB protein is the loading control. (**c**) Bar graph demonstrating FOXP4 protein levels after transfection with siRNA. (**d**) The CCK-8 assay showing the proliferations of human SSCs transfected with NC-siRNA and *FOXP4*-siRNA1. (**e**) PCNA protein levels in human SSCs after transfections with NC-siRNA and *FOXP4*-siRNA1. (**f**) Bar graph illustrating the down-regulation of PCNA protein after transfection with *FOXP4*-siRNA1. (**g**) Proportions of EdU-positive cells after transfection of human SSCs with NC-siRNA and *FOXP4*-siRNA1. Scale bars = 50 μm. (**h**) Bar graph showing changes in the proportion of EdU-positive cells after transfection with *FOXP4*-siRNA1. FOXP4: forkhead box P4; NC-siRNA: negative control siRNA; siRNA: small interfering RNA; PCNA: proliferating cell nuclear antigen; EdU: 5-ethynyl-2'-deoxyuridine; RT-qPCR: real-time quantitative polymerase chain reaction; OD: optical density; CCK8: cell counting kit-8. DAPI: 4',6-diamidino-2-phenylindole; ACTB: beta-actin. $^{*}P < 0.05$, comparison between *FOXP4*-siRNA1 and NC-siRNA groups.

RESULTS

Gene expression in human spermatogonia

To assess the mechanisms regulating human SSC development, we analyzed scRNA-seq datasets (GSE149512 and GSE112013) of the adult testes with normal spermatogenesis. Screening and integration of data led to identification of 5176 testicular cells and 23 125 genes. "Seurat" in R was used to reduce data dimensionality, which divided the cells into 13 populations (**Figure 1a** and **1b**, and **Supplementary Table 4**). Then, we quantified the levels of common testicular cell marker genes, including SSC markers (inhibitor of DNA binding 4 [*ID*4]), differentiation markers (KIT proto-oncogene, receptor tyrosine kinase [*KIT*] and stimulated by retinoic acid gene 8 [*STRA*8]), meiosis markers (synaptonemal complex protein 1 [*SYCP*1], meiosis-specific with OB domain-containing [*MEIOB*], and proteasome subunit alpha type-8 [*PSMA*8]), spermatid structure proteins (nuclear transition protein 2 [*TNP*2]), and some somatic markers. These markers were used to identify particular cell populations (**Figure 1b**). These 13 cell populations were SSCs, differentiating spermatogonia (Diff. ing Spg), leptotene spermatocytes (L), zygotene spermatocytes (Z), pachytene/diplotene (P/D) spermatocytes, round or elongated spermatids (RS1, RS2, ES1, and ES2), Leydig cells (LCs), Sertoli cells (SCs)/endothelial cells (ECs), peritubular myoid cells (PTM)/Leydig cells/endothelial cells, and macrophages (Mø). In addition, SSC marker genes in all populations were analyzed using "Seurat" in R. Moreover, Gene Ontology (GO) terms of the top 500 differentially expressed genes were analyzed (**Supplementary Table 5**). The SSC cluster was found to be enriched in "RNA splicing" and "Ribonucleoprotein complex biogenesis" terms, indicating that this cluster was undergoing active

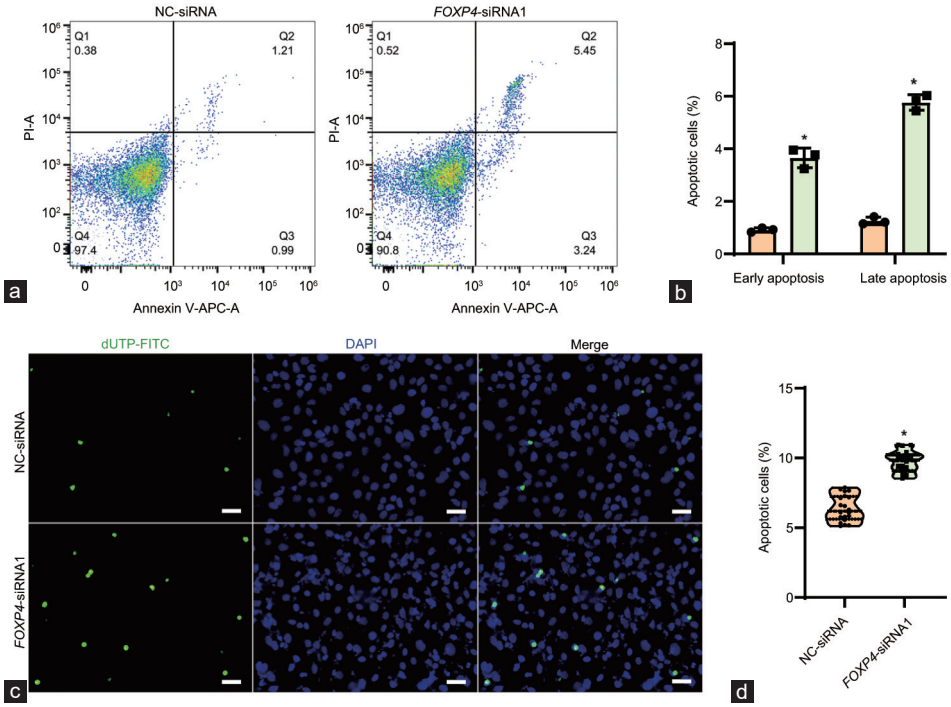

Figure 4: Effects of FOXP4 suppression on human SSC apoptosis. (**a**) Flow cytometry and FITC Annexin V analysis showing proportions of early and late apoptotic cells in human SSCs transfected with NC-siRNA and *FOXP4*-siRNA1. (**b**) Bar graph demonstrating the changes in early and late apoptosis in **a** after transfection with *FOXP4*-siRNA1. (**c**) TUNEL analysis showing proportions of TUNEL-positive cells in human SSCs transfected with NC-siRNA and *FOXP4*-siRNA1. Scale bars = 50 μm. (**d**) Violin plot exhibiting changes of TUNEL-positive cells in **c** after knockdown of *FOXP4*. FOXP4: forkhead box P4; NC-siRNA: negative control siRNA; siRNA: small interfering RNA; SSC: spermatogonial stem cell; TUNEL: terminal deoxynucleotidyl transferase (TdT)-mediated dUTP nick-end labeling; PI: propidium iodide; DAPI: 4',6-diamidino-2-phenylindole; ACTB: beta-actin; APC: allophycocyanin; dUTP: 2'-deoxyuridine 5'-triphosphate; FITC: flourescein isothiocyanate. $^*P < 0.05$ indicates significant differences between *FOXP4*-siRNA1 and NC-siRNA groups.

transcriptional translation (**Figure 1c** and **Supplementary Table 6**). Moreover, several genes were dominantly expressed in human SSCs. To analyze the regulation of SSCs, SSC clusters were subjected to in-depth analysis and further subdivided into two clusters; State 0 and State 1 (**Figure 1d** and **Supplementary Table 7**). Using "monocle" in R, a quasi-chronological analysis of cells was performed to determine their developmental trajectories. Based on expression levels of undifferentiated spermatogonia marker genes (*GFRA*1 and *ID*4), it was established that State 0 was the developmental starting point (**Figure 1e**). Several genes, including *FOXP*4, chromosome 18 C19orf84 homolog (*C*19*orf*84), cystatin-3 (*CST*3), guanine nucleotide-binding protein subunit beta-2-like 1 (*GNB*2*L*1), melanoma-associated antigen B2 (*MAGEB*2), and *ID*4 were differentially expressed between State 0 and State 1. Genes in the top 10 differentially expressed genes were analyzed pseudo-chronologically (**Figure 1f** and **1g**). Among the genes, *FOXP*4 expression gradually increased during SSC development, implying that FOXP4 may have an important role in SSC fate regulation.

FOXP4 is highly expressed in human SSCs

To confirm the above findings, we examined protein expression in human testicular tissues. Specifically, FOXP4 protein levels in testis samples from three OA patients with normal spermatogenesis were determined by Western blot (**Figure 2a**). The analysis of FOXP4 localization in OA samples with normal spermatogenesis revealed that FOXP4 was mainly localized in the nuclei of cells near the seminiferous tubule basement membrane, suggesting that it is expressed in spermatogonia (**Figure 2b** and **2c**). Cell subtypes in at least 20 seminiferous tubule sections in which FOXP4 was expressed were also determined by double immunofluorescence (**Figure 2d**). FOXP4 was coexpressed with GFRA1 (a marker of SSCs) in 82.5% (s.d.: 3.7%) of cells. However, only 6.6% FOXP4-positive cells expressed KIT, a marker for differentiating spermatogonia. Almost all FOXP4-positive cells expressed proliferating cell nuclear antigen (PCNA), a marker for cell proliferation and DNA damage repair (**Figure 2e**). Given that spermatogonia are less frequently subjected to DNA damage repair in the normal state, these results imply that FOXP4 may influence human SSC proliferation. These data are consistent with the results from bioinformatic analysis.

FOXP4 knockdown and human SSC proliferation

To assess the significance of FOXP4 in regulation of SSCs, a human SSC line with similar biological characteristics to primary human SSC was used. We inhibited *FOXP4* expression in human SSCs by siRNA. The success of *FOXP4* knockdown was confirmed by RT-qPCR and Western blot (**Figure 3a**–**3c**). Since *FOXP4*-siRNA1 had the best knockdown efficiency, it was used to repress FOXP4 expression in SSCs. Effects of FOXP4 inhibition on cell proliferations were determined via the CCK-8 assay. *FOXP4* knockdown suppressed human SSC proliferation from days 2 to 5 (**Figure 3d**). Moreover, PCNA (a marker of cell proliferation) protein levels were markedly suppressed upon *FOXP4* knockdown (**Figure 3e** and **3f**). EdU analysis of DNA synthesis at 48 h after transfection revealed that the abundance of EdU-positive cells was markedly reduced in FOXP4-repressed cells, compared with negative controls (35.7% ± 0.6% *vs* 22.1% ± 1.6%, $P < 0.05$; **Figure 3g** and **3h**). Thus, FOXP4 enhances human SSC growth and DNA synthesis.

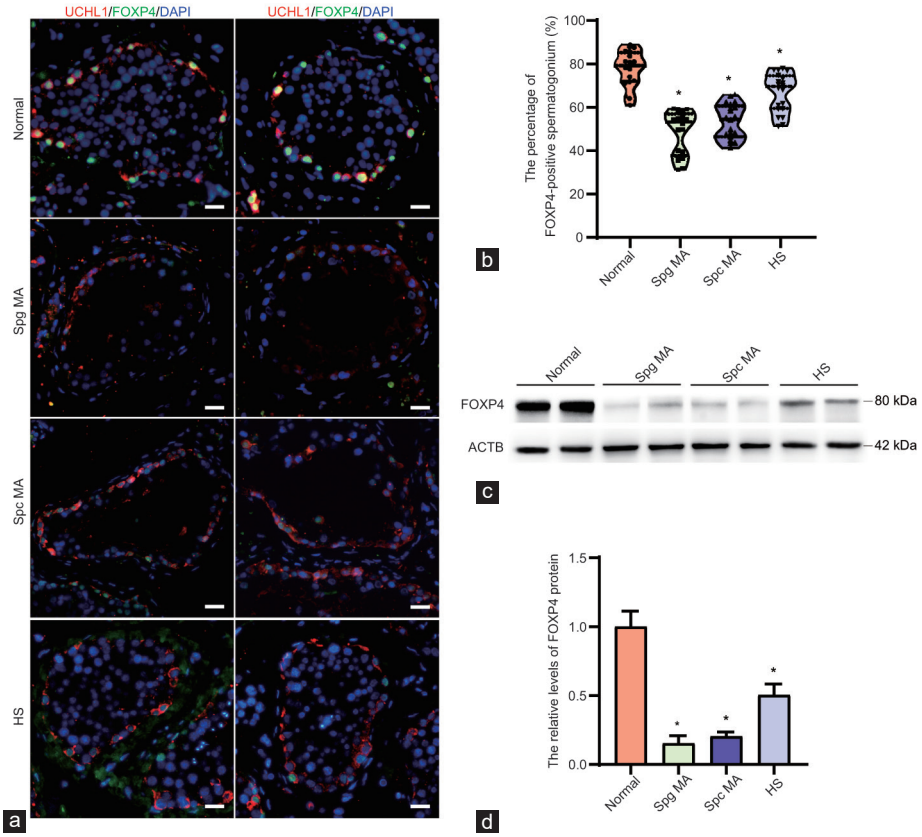

Figure 5: FOXP4 expressions in testes of OA and NOA patients. (**a**) Two-color immunofluorescence to explore the distribution of UCHL1-positive SSCs (red) with FOXP4 expressions (green) in OA and other types of NOA patients. Each picture represents one testicular sample. Each group had two samples. Scale bars = 50 μm. (**b**) Violin plot showing the proportion of double positive cells in different types of testes in **a**. (**c**) Western blot results showing FOXP4 protein levels in OA and NOA patients. (**d**) Bar graph describing the difference in FOXP4 protein levels between different testicular samples in **c**. Normal: normal spermatogenesis; Spg MA: spermatogonia maturation arrest; Spc MA: spermatocyte maturation arrest; FOXP4: forkhead box P4; SSC: spermatogonial stem cell; OA: obstructive azoospermia; NOA: nonobstructive azoospermia; HS: hypospermatogenesis; UCHL1: ubiquitin carboxyl-terminal hydrolase isozyme L1; DAPI: 4',6-diamidino-2-phenylindole. $^*P < 0.05$ indicates significant differences between OA patients with normal spermatogenesis and NOA patients.

***FOXP4* deficiency and apoptosis in human SSCs**

Given that *FOXP4* knockdown markedly increased cell debris during cell cultures, we assessed its effects on cell apoptosis via Annexin V/PI staining and Flow cytometry. Both early and late apoptotic rates were significantly increased in the *FOXP4* knockdown group, relative to negative control (NC) group (early apoptosis: 3.7% ± 0.4% *vs* 0.9% ± 0.1%, $P < 0.05$; late apoptosis: 5.8% ± 0.3% *vs* 1.3% ± 0.1%, $P < 0.05$; **Figure 4a** and **4b**). The TUNEL assay revealed a significantly higher abundance of TUNEL positive cells after *FOXP4* knockdown, than in the negative control (NC) group (median [interquartile range]: 9.9% [9.1%–10.2%] *vs* 6.2% [5.6%–7.3%], $P < 0.05$; **Figure 4c** and **4d**). Therefore, FOXP4 repression induced human SSC apoptosis.

***FOXP4* downregulation and correlation with spermatogenic failure in NOA**

NOA is a severe male infertility disorder. From testicular histopathological features, NOA with failure in spermatogenesis is categorized as following subtypes: spermatid maturation arrest (Std MA), spermatocyte maturation arrest (Spc MA), spermatogonia maturation arrest (Spg MA), hypospermatogenesis (HS) and SCOS. To evaluate the relationship between FOXP4 levels and dysregulated spermatogenesis, testicular tissues from eight patients were obtained for histopathological assessment (**Supplementary Figure 1**). The spermatogenesis status of testes was evaluated by H&E staining. Examination of FOXP4 expression (green) and localization in SSCs by coimmunohistochemistry with UCHL1 (red) showed that FOXP4-positive SSC abundance was markedly lower in Spg MA, Spc MA, and HS samples, relative to samples with normal spermatogenesis, and that fluorescence intensities were also decreased in those samples (**Figure 5a** and **5b**). Western blot analysis revealed that FOXP4 levels were markedly suppressed in all samples with dysregulated spermatogenesis (**Figure 5c** and **5d**). These results indicate that aberrant FOXP4 expressions are correlated with spermatogenic disorders, particularly spermatogonia and spermatocyte maturation.

DISCUSSION

Biologically, SSCs are involved in maintenance of adult spermatogenesis. However, owing to species differences and limited availability of human samples, developmental regulation of SSCs in humans has not been fully established. In 1994, Brinster and Avarbock[3] restored spermatogenesis in recipient mice by transplanting mouse spermatogonia. However, owing to limitations in *in vitro* expansion and culture of human SSCs,[4] a similar approach could not be used to restore human spermatogenesis by using stem cells. Thus, elucidation of mechanisms that regulate human SSC development, particularly their self-renewal and proliferation, is urgently needed. Advances in single-cell sequencing technology have permitted better understanding of developmental processes of human SSCs at the single-cell level and

identification of involved regulatory mechanisms.[32,43] By analyzing published single-cell sequencing data from adult human testes with normal spermatogenesis, we found that FOXP4 was differentially expressed in human SSCs and that its expression gradually increased with SSC development, indicating that FOXP4 is associated with SSC activation and proliferation.

The FOXP protein subfamily belongs to the FOX family of transcription factors, which regulate vital developmental processes in several organ systems, such as the pulmonary, nervous, cardiac, reproductive, and immune.[33] The FOXP family comprises FOXP1 (3p14.1), FOXP3 (Xp11.23), FOXP2 (7q31), and FOXP4 (6p21.1) that exhibit a 110-amino acid DNA-binding domain referred to as the winged helix/forkhead domain.[44] In humans, *FOXP3* mutations cause male infertility by affecting the functions of SSCs.[45] FOXO1, a member of the FOX family, affects SSC self-renewal and differentiation in mice by regulating the functions of proto-oncogene tyrosine-protein kinase receptor Ret.[46] FOXP4 was first discovered in the lungs and intestines,[35] and its roles in development of lungs, immune, and nervous systems have been evaluated. FOXP4 deletion is associated with severe cardiac defects that result in embryonic lethality at embryonic days 10.5–12.5.[34] During nerve system development, suppressed FOXP4 levels lead to various neural tube defects.[34] FOXP4 inhibits N-cadherin, a key constituent of adherent junctions between neural progenitors, and promotes neural differentiation by counteracting progenitor maintenance activities of SOX2.[47] During tumor development, miR-138, miR-338-3p, and miR-4316 inhibit tumor cell proliferation, migration, and invasion through FOXP4.[48] Moreover, FOXP4 affects cell proliferation by regulating the WNT pathway.[49] Our results showed that *FOXP4* knockdown suppresses SSC proliferation and enhances their apoptosis. However, the associated regulatory mechanisms of FOXP4 have not been conclusively determined. Given that the WNT pathway also regulates SSC proliferation, the association between FOXP4 and WNT signaling should be investigated.

We divided all testicular cells into 13 clusters, with little differences from other reports.[43,50] STRA8 is a marker for differentiated spermatogonia;[51] however, differentiated spermatogonia were not distinguished in this study. During data quality control, we selectively removed a large number of cells with mitochondrial genes higher than 15%, which may have led to a small number of *STRA8*-positive differentiated spermatogonia, without being separately clustered. We further divided SSCs into two different states, and this also differs from other reports. Guo *et al*.[32] reported that SSCs and differentiating spermatogonia can be divided into five states. Sohni *et al*.[43] divided all spermatogonia into five states, while Zhao *et al*.[31] divided SSCs into three states. This may be because, to achieve data dimensionality reduction, we chose different resolution parameters and reduction methods. Alternatively, we integrated two datasets, and batch effects between them may have had an impact on clustering results.

Human spermatogenesis is maintained by SSCs, and the functions of spermatogonia can affect spermatogenesis.[5] In mice, impaired functions of SSCs cause abnormal spermatogenesis and, in severe cases, the complete loss of germ cells.[18] Although we demonstrated the roles of FOXP4 in SSC proliferation and apoptosis *in vitro*, we did not establish whether the loss of FOXP4 impairs spermatogenesis. For our analyses, we obtained testes in different spermatogenic states, including normal, spermatogonial maturation arrest, spermatocyte maturation arrest, and hypospermatogenesis. Expression levels and positive percentage of FOXP4 were significantly downregulated in NOA testicular tissues, implying that abnormal expressions of FOXP4 may be associated with dysregulated spermatogenesis. However, the causal relationship between FOXP4 deficiency and abnormal spermatogenesis should be investigated further. To confirm its roles in human spermatogenesis, it is necessary to search for *FOXP4* mutations in patients with abnormal spermatogenesis.

CONCLUSION

In summary, FOXP4 is highly expressed in human SSCs and its deficiency suppresses DNA synthesis and cell proliferation and significantly induces apoptosis. In testes with abnormal spermatogenesis, FOXP4 expression is significantly downregulated. Our findings reveal the pathways and genes involved in the regulation of SSC fates in humans and uncover the molecular targets that can be used for male infertility diagnosis and treatment.

AUTHOR CONTRIBUTIONS

LQF designed the study and supervised all experiments. SWL and LT performed the experiments and drafted the manuscript. DZ and HB assisted with experimental procedures and sample collection. All authors read and approved the final manuscript.

COMPETING INTERESTS

All authors declare no competing interests.

ACKNOWLEDGMENTS

The authors thank Zuping He of Hunan Normal University (Changsha, China) for providing the human spermatogonia stem cell line. This study was supported by the grants from the Scientific Research Planning Project of Hunan Provincial Health and Family Planning Commission (B2017143), the Natural Science Foundation of Changsha (kq2202491), and the Research Grant of CITIC-Xiangya (YNXM 202109 and YNXM 202115).

Supplementary Information is linked to the online version of the paper on the *Asian Journal of Andrology* website.

REFERENCES

1 Qiao J, Wang Y, Li X, Jiang F, Zhang Y, *et al.* A Lancet commission on 70 years of women's reproductive, maternal, newborn, child, and adolescent health in China. *Lancet* 2021; 397: 2497–536.
2 Corona G, Minhas S, Giwercman A, Bettocchi C, Dinkelman-Smit M, *et al.* Sperm recovery and ICSI outcomes in men with non-obstructive azoospermia: a systematic review and meta-analysis. *Hum Reprod Update* 2019; 25: 733–57.
3 Brinster RL, Avarbock MR. Germline transmission of donor haplotype following spermatogonial transplantation. *Proc Natl Acad Sci U S A* 1994; 91: 11303–7.
4 Medrano JV, Rombaut C, Simon C, Pellicer A, Goossens E. Human spermatogonial stem cells display limited proliferation *in vitro* under mouse spermatogonial stem cell culture conditions. *Fertil Steril* 2016; 106: 1539–49.e8.
5 de Rooij DG, Russell LD. All you wanted to know about spermatogonia but were afraid to ask. *J Androl* 2000; 21: 776–98.
6 Di Persio S, Saracino R, Fera S, Muciaccia B, Esposito V, *et al.* Spermatogonial kinetics in humans. *Development* 2017; 144: 3430–9.
7 de Rooij DG. The nature and dynamics of spermatogonial stem cells. *Development* 2017; 144: 3022–30.
8 Meng X, Lindahl M, Hyvönen ME, Parvinen M, de Rooij DG, *et al.* Regulation of cell fate decision of undifferentiated spermatogonia by GDNF. *Science* 2000; 287: 1489–93.
9 Masaki K, Sakai M, Kuroki S, Jo JI, Hoshina K, *et al.* FGF2 has distinct molecular functions from GDNF in the mouse germline niche. *Stem Cell Reports* 2018; 10: 1782–92.
10 Lee J, Kanatsu-Shinohara M, Morimoto H, Kazuki Y, Takashima S, *et al.* Genetic reconstruction of mouse spermatogonial stem cell self-renewal *in vitro* by Ras-cyclin D2 activation. *Cell Stem Cell* 2009; 5: 76–86.
11 Oatley JM, Avarbock MR, Brinster RL. Glial cell line-derived neurotrophic factor regulation of genes essential for self-renewal of mouse spermatogonial stem cells is dependent on Src family kinase signaling. *J Biol Chem* 2007; 282: 25842.
12 He Z, Jiang J, Kokkinaki M, Golestaneh N, Hofmann MC, *et al.* GDNF induces CREB-1, ATF-1, and CREM-1 phosphorylation and up-regulates *c-fos* transcription via the Ras/ERK1/2 pathway to promote mouse spermatogonial stem cell proliferation. *Stem Cells* 2008; 26: 266.

13 Ishii K, Kanatsushinohara M, Toyokuni S, Shinohara T. FGF2 mediates mouse spermatogonial stem cell self-renewal via upregulation of *Etv5* and *Bcl6b* through MAP2K1 activation. *Development* 2012; 139: 1734.
14 La HM, Mäkelä JA, Chan AL, Rossello FJ, Nefzger CM, *et al*. Identification of dynamic undifferentiated cell states within the male germline. *Nat Commun* 2018; 9: 2819.
15 La HM, Hobbs RM. Mechanisms regulating mammalian spermatogenesis and fertility recovery following germ cell depletion. *Cell Mol Life Sci* 2019; 76: 4071–102.
16 Yang QE, Kim D, Kaucher A, Oatley MJ, Oatley JM. CXCL12-CXCR4 signaling is required for the maintenance of mouse spermatogonial stem cells. *J Cell Sci* 2013; 126: 1009–20.
17 Makela JA, Hobbs RM. Molecular regulation of spermatogonial stem cell renewal and differentiation. *Reproduction* 2019; 158: R169–87.
18 Buaas FW, Kirsh AL, Sharma M, McLean DJ, Morris JL, *et al*. Plzf is required in adult male germ cells for stem cell self-renewal. *Nat Genet* 2004; 36: 647–52.
19 Lovelace DL, Gao Z, Mutoji K, Song YC, Ruan J, *et al*. The regulatory repertoire of PLZF and SALL4 in undifferentiated spermatogonia. *Development* 2016; 143: 1893–906.
20 Hobbs RM, Marco S, Ilaria F, Shahin R, Pier Paolo P. Plzf regulates germline progenitor self-renewal by opposing mTORC1. *Cell* 2010; 142: 468–79.
21 Huckins C. The spermatogonial stem cell population in adult rats. I. Their morphology, proliferation and maturation. *Anat Rec* 1971; 169: 533–57.
22 Lord T, Oatley JM. A revised A_{single} model to explain stem cell dynamics in the mouse male germline. *Reproduction* 2017; 154: R55–64.
23 Hara K, Nakagawa T, Enomoto H, Suzuki M, Yamamoto M, *et al*. Mouse spermatogenic stem cells continually interconvert between equipotent singly isolated and syncytial states. *Cell Stem Cell* 2014; 14: 658–72.
24 Rowley MJ, Berlin JD, Heller CG. The ultrastructure of four types of human spermatogonia. *Z Zellforsch Mikrosk Anat* 1971; 112: 139–57.
25 Johnson L. A new approach to study the architectural arrangement of spermatogenic stages revealed little evidence of a partial wave along the length of human seminiferous tubules. *J Androl* 1994; 15: 435–41.
26 Muciaccia B, Boitani C, Berloco BP, Nudo F, Spadetta G, *et al*. Novel stage classification of human spermatogenesis based on acrosome development. *Biol Reprod* 2013; 89: 60.
27 Guo J, Grow EJ, Yi C, Mlcochova H, Maher GJ, *et al*. Chromatin and single-cell RNA-Seq profiling reveal dynamic signaling and metabolic transitions during human spermatogonial stem cell development. *Cell Stem Cell* 2017; 21: 533–46.e6.
28 Hermann BP, Sukhwani M, Hansel MC, Orwig KE. Spermatogonial stem cells in higher primates: are there differences to those in rodents? *Reproduction* 2010; 139: 479.
29 Zhou D, Wang X, Liu Z, Huang Z, Nie H, *et al*. The expression characteristics of FBXW7 in human testis suggest its function is different from that in mice. *Tissue Cell* 2020; 62: 101315.
30 Kanatsu-Shinohara M, Onoyama I, Nakayama KI, Shinohara T. Skp1-Cullin-F-box (SCF)-type ubiquitin ligase FBXW7 negatively regulates spermatogonial stem cell self-renewal. *Proc Natl Acad Sci U S A* 2014; 111: 8826–31.
31 Zhao L, Yao C, Xing X, Jing T, Li P, *et al*. Single-cell analysis of developing and azoospermia human testicles reveals central role of Sertoli cells. *Nat Commun* 2020; 11: 5683.
32 Guo J, Grow EJ, Mlcochova H, Maher GJ, Lindskog C, *et al*. The adult human testis transcriptional cell atlas. *Cell Res* 2018; 28: 1141–57.
33 Kim JH, Hwang J, Jung JH, Lee HJ, Lee DY, *et al*. Molecular networks of FOXP family: dual biologic functions, interplay with other molecules and clinical implications in cancer progression. *Mol Cancer* 2019; 18: 180.
34 Co M, Anderson AG, Konopka G. FOXP transcription factors in vertebrate brain development, function, and disorders. *Wiley Interdiscip Rev Dev Biol* 2020; 9: e375.
35 Lu MM, Li S, Yang H, Morrisey EE. Foxp4: a novel member of the Foxp subfamily of winged-helix genes co-expressed with Foxp1 and Foxp2 in pulmonary and gut tissues. *Mech Dev* 2002; 119 Suppl 1: S197–202.
36 Shu W, Yang H, Zhang L, Lu MM, Morrisey EE. Characterization of a new subfamily of winged-helix/forkhead (Fox) genes that are expressed in the lung and act as transcriptional repressors. *J Biol Chem* 2001; 276: 27488–97.
37 Qi W, Gao C, Zhang L, Gao Z, Sui J, *et al*. MiR-3196, a p53-responsive microRNA, functions as a tumor suppressor in hepatocellular carcinoma by targeting FOXP4. *Am J Cancer Res* 2019; 9: 2665–78.
38 Yang L, Liu Z, Ma J, Wang H, Gao D, *et al*. CircRPPH1 serves as a sponge for miR-296-5p to enhance progression of breast cancer by regulating FOXP4 expression. *Am J Transl Res* 2021; 13: 7556–73.
39 Niu Y, Wang G, Li Y, Guo W, Guo Y, *et al*. LncRNA FOXP4-AS1 promotes the progression of esophageal squamous cell carcinoma by interacting with MLL2/H3K4me3 to upregulate FOXP4. *Front Oncol* 2021; 11: 773864.
40 Tam WY, Leung CK, Tong KK, Kwan KM. Foxp4 is essential in maintenance of Purkinje cell dendritic arborization in the mouse cerebellum. *Neuroscience* 2011; 172: 562–71.
41 Hou J, Niu M, Liu L, Zhu Z, Wang X, *et al*. Establishment and characterization of human germline stem cell line with unlimited proliferation potentials and no tumor formation. *Sci Rep* 2015; 5: 16922.
42 Zhou D, Fan J, Liu Z, Tang R, Wang X, *et al*. TCF3 regulates the proliferation and apoptosis of human spermatogonial stem cells by targeting PODXL. *Front Cell Dev Biol* 2021; 9: 695545.
43 Sohni A, Tan K, Song HW, Burow D, de Rooij DG, *et al*. The neonatal and adult human testis defined at the single-cell level. *Cell Rep* 2019; 26: 1501–17.e4.
44 Santos ME, Athanasiadis A, Leitão AB, DuPasquier L, Sucena E. Alternative splicing and gene duplication in the evolution of the *FoxP* gene subfamily. *Mol Biol Evol* 2011; 28: 237–47.
45 Qiu Q, Yu X, Yao C, Hao Y, Fan L, *et al*. FOXP3 pathogenic variants cause male infertility through affecting the proliferation and apoptosis of human spermatogonial stem cells. *Aging* 2019; 11: 12581–99.
46 Goertz MJ, Zhuoru W, Gallardo TD, Kent HF, Castrillon DH. Foxo1 is required in mouse spermatogonial stem cells for their maintenance and the initiation of spermatogenesis. *J Clin Invest* 2011; 121: 3456.
47 Rousso DL, Pearson CA, Gaber ZB, Miquelajauregui A, Li S, *et al*. Foxp-mediated suppression of N-cadherin regulates neuroepithelial character and progenitor maintenance in the CNS. *Neuron* 2012; 74: 314–30.
48 Wang N, Gu Y, Li L, Wang F, Lv P, *et al*. Circular RNA circMYO9B facilitates breast cancer cell proliferation and invasiveness via upregulating FOXP4 expression by sponging miR-4316. *Arch Biochem Biophys* 2018; 653: 63–70.
49 Shi J, Wang J, Cheng H, Liu S, Hao X, *et al*. FOXP4 promotes laryngeal squamous cell carcinoma progression through directly targeting LEF-1. *Mol Med Rep* 2021; 24: 831.
50 Wang M, Liu X, Chang G, Chen Y, An G, *et al*. Single-cell RNA sequencing analysis reveals sequential cell fate transition during human spermatogenesis. *Cell Stem Cell* 2018; 23: 599–614.e4.
51 Zhou Q, Li Y, Nie R, Friel P, Mitchell D, *et al*. Expression of stimulated by retinoic acid gene 8 (Stra8) and maturation of murine gonocytes and spermatogonia induced by retinoic acid *in vitro*. *Biol Reprod* 2008; 78: 537–45.

Supplementary Table 1: The primers used for real-time polymerase chain reaction and reverse transcription polymerase chain reaction

Genes	*Primer sequences (5'-3')*	*Product sizes (bp)*
FOXP4	F: GACAGCCTACTGTGCTCACAT	91
	R: TTGCACTCTCCGTGTCCGTA	
ACTB	F：CGCACCACTGGCATTGTCAT	206
	R: TTCTCCTTGATGTCACGCAC	

F: forward primer; R: reverse primer; *FOXP4*: forkhead box P4; *ACTB*: beta-actin

Supplementary Table 2: Antibodies applied in Western blots, immunofluorescence and immunoprecipitation

Antibodies	*Source*	*Dilution*	*Incubation*
Western blot			
FOXP4	Abcam cat#ab17726	1:600	12 h at 4°C
Immunofluorescence			
FOXP4	Abcam cat#ab17726	1:200	12–16 h at 4°C
UCHL1	Abcam cat#ab8189	1:50	16 h at 4°C
GFRα1	R&Dcat#AF560	1:25	16 h at 4°C
PCNA	Abcam cat#ab29	1:50	12–16 h at 4°C
KIT	R and D cat#AF332	1:25	16 h at 4°C
Secondary antibody			
Donkey anti-Rabbit IgG, Alexa Fluor 488	Thermo Fisher Scientific cat#A21206	1:1000	1 h at 25°C
Donkey anti-Mouse IgG, Alexa Fluor 594	Thermo Fisher Scientific cat#A21203	1:1000	1 h at 25°C
Donkey anti-Goat IgG, Alexa Fluor 594	Thermo Fisher Scientific cat#A11058	1:1000	1 h at 25°C

FOXP4: forkhead box P4; PCNA: proliferating cell nuclear antigen; KIT: KIT proto-oncogene, receptor tyrosine kinase

Supplementary Table 3: The small interfering RNA sequences targeting human forkhead box P4 mRNA

siRNA	*Targeting sequence*
FOXP4-siRNA1	CCGGATCACTCAAGCAATA
FOXP4-siRNA2	GAACCTGAATCCCAAAGCA
FOXP4-siRNA3	AGCCTCTCTTCATCCACAT

siRNA: small interfering RNA; FOXP4: forkhead box P4

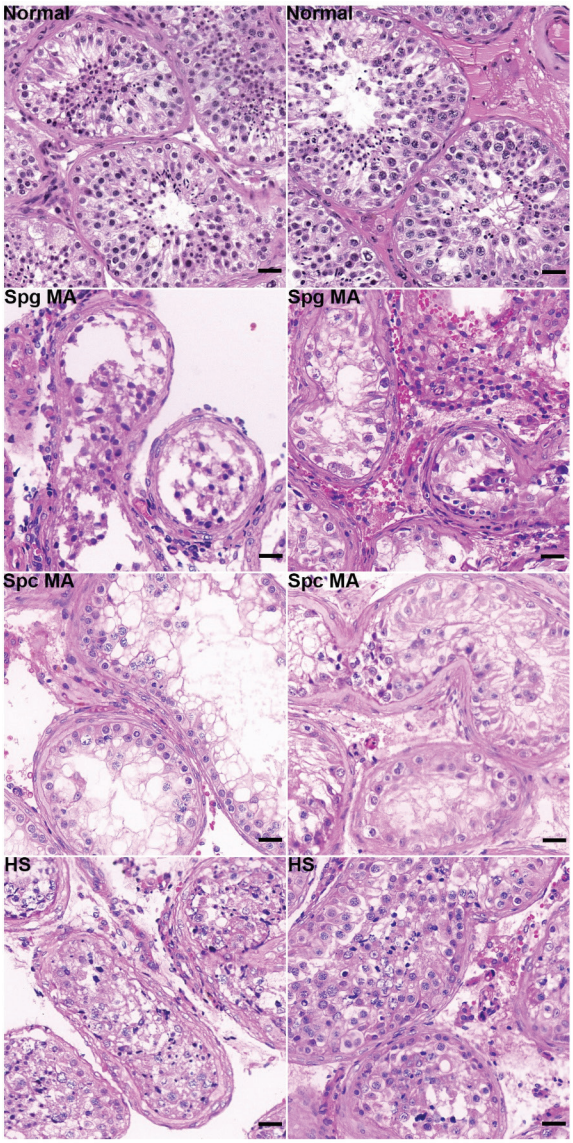

Supplementary Figure 1: HE staining for 8 testicular tissues with different spermatogenic status. All samples were classified as normal, Spg MA, Spc MA, and HS according to the Johnsen score. Scale bars, 50 μm. Spg MA: spermatogonia maturation arrest; Spc MA: spermatocyte maturation arrest; HS: hypospermatogenesis; HE: hematoxylin and eosin.